Evaluating the climatic response to changes in CO_2 and solar luminosity

Zavareh Kothavala[1], Robert J. Oglesby[2] and B. Saltzman[1]

[1] *Department of Geology and Geophysics, Yale University, New Haven, CT 06520 USA.*
[2] *Department of Earth and Atmospheric Sciences, Purdue University, West Lafayette, IN 47907 USA.*

Abstract A series of simulations was conducted using the latest version of the NCAR Community Climate Model (CCM3) to investigate the equilibrium response of surface temperature and other key variables to atmospheric CO_2 concentrations and varied solar luminosity. The CCM3 is a general circulation model (GCM) of the Earth's global climate. Eight GCM simulations with CO_2 concentrations of 180, 230, 355, 710, 1000, 2000 and 3000 ppmv were run for a minimum of thirty two seasonal cycles each. The 355 ppmv simulation with a solar constatn of 1367 W m^{-2} was designated as the control run for the present-day climate. The results showed the same basic non-linear behavior of temperature to CO_2 concentrations obtained previously with a similarly designed experiment with CCM1, an earlier version of the NCAR GCM. The magnitude of the sensitivities, however, were much lower in the new CCM3 runs than in the older CCM1 runs. An additional four GCM simulations with a CO_2 concentration fixed at 355 ppmv and solar luminosity values of +5%, +2%, -2% and -5% of (the present day value of) 1367 watts per meter square have been completed. Results of these latter experiments yield a more linear response than to the changes in CO_2, although more detailed analyses are currently in progress.

1. Introduction

The prolific use of Global Climate Models (GCMs) to study past and future climate change [4] requires an understanding of the sensitivity of the fast response variables of the model to external forcing. With respect to such an atmospheric GCM, the key external forcing factors include (a) short-wave solar luminosity forcing, (b) long wave CO_2 forcing, and (c) storage of heat in the deep ocean. Milankavitch insolation variations resulting from variations through orbital and precession changes, affect the model through the duration and amount of short-wave radiation reaching the surface in a year. Numerous studies of model sensitivity to CO_2 forcing have been conducted using different GCMs [11, 13, 12, 7]. However, fewer studies have examined the effects of the model to solar luminosity changes [5, 8, 13] and fewer still to the forcing due to the deep ocean temperature (a study based on a statistical-dynamical model is given in [10]). The objective of this study is to examine the model sensitivity to CO_2 and solar luminosity using a recent GCM.

The properties of the GCM are reviewed in Section 2 and the experiments are described in Section 3. The GCM simulation of surface temperature is evaluated in Section 4 and the sensitivity to CO_2 and solar luminosity in Section 5. Spatial patterns of temperature anomalies between the present day simulation and the extreme values of CO_2 and solar luminosity are presented in Section 6.

2. Model description

The GCM examined in this paper, CCM3, was developed at the National Center for Atmospheric Research (NCAR) as a derivative of the Community Climate Model series. This spectral model has a T42 (2.8° longitude × 2.8° latitude) horizontal resolution. This resolution translates to 64 grid points in latitude and 128 grid points in longitude. CCM3 has eighteen vertical levels, the LSM land-surface package [2] and includes the seasonal and diurnal cycle of radiation. The model is fully described by [6], with results and comparisons to observations given by [3].

3. Experiment design

The eight values of CO_2 employed are 180 ppmv, 230 ppmv, 355 ppmv, 530 ppmv, 710 ppmv, 1000 ppmv, 2000 ppmv and 3000 ppmv. The 355 ppmv corresponds to the present day concentration of CO_2 in the atmosphere [4] and represents the control climate in our suite of runs. The 180 ppmv simulation is similar to CO_2 concentrations during the Last Glacial Maximum and the 230 ppmv simulation corresponds to the Younger Dryas period. The 710 ppmv simulation is the double CO_2 scenario that is commonly analyzed in climate change scenarios and the 1000 ppmv is close to thrice the present day values, also used in the study of extreme events. The 530 ppmv simulation, has a CO_2 concentration between the present day and doubled CO_2 values and could represent the Pliocene epoch. The higher values of 2000 ppmv and 3000 ppmv represent possible warmer earth scenarios of the early Cenozoic and Mesozoic [1]. All CO_2 simulations were run out to at least 32 model years with the solar constant fixed at 1367 W m^{-2}.

In order to examine the sensitivity of the model to changes in shortwave forcing, four additional experiments were conducted by varying the solar constant between -5% and +5% of the present day value as listed in Table 1. Although paleo analogs exist for a solar luminosity lower

Table 1: Solar luminosity simulations

Experiment number	Relative Change	Absolute value Wm^{-2}	Length (years)
1	-5%	1299	27
2	-2%	1340	27
3	none	1367	39
4	+2%	1394	27
5	+5%	1435	27

than a present day value, there are no paleo analogs for an increase in the solar constant.

4. Model evaluation

Figure 1 shows the twelve-month running mean of the global-average surface temperatures of the CO_2 sensitivity model runs over the final eleven model years (final ten model years for the 230 ppmv run). The present-day global average temperature of the control simulation (355 ppmv) is 287.5 K and the difference (model sensitivity) between present-day and doubled CO_2 (710 ppm) conditions is 2.3K. This value is consistent with the coupled ocean-atmosphere GCMs evaluated in the most recent Intergovernmental Panel of Climate Change (IPCC) report [4]. Figure 2 shows the twelve month running mean over the last ten years of the control run and the four additional solar constant sensitivity experiments.

Although a normalized comparison of the change in surface temperature between the two sets of experiments would be the most appropriate, a general comparison of the ranges between the selected perturbations are presented. The twelve month running mean for the CO_2 experiments ranged between 285K and 296K, and for the solar constant runs and between 279K and 295K. The 2.3K sensitivity with the doubling of CO_2 can be surpassed with a 2% increase in the solar constant (equivalent to about 27 W m^{-2} leading to a change of about 3K). Increasing the solar constant by 5% yielded an 8K increase in surface temperature but decreasing the solar constant by 5% yielded a 9K decrease, possibly because of snow and sea-ice albedo feedback processes. The global average temperature of 295K from the +5% can only be achieved with a CO_2 concentration of 2000 ppmv. At the other extreme, it was not possible to set the CO_2 concentration in CCM3 low enough to achieve the global average temperature of 279K obtained with the -5% decrease in solar luminosity. Although the reasons for this are still unclear, we suspect the model becomes too cold in the upper polar atmosphere.

The GCM simulations of temperature and snow for the months of June, July and August will be the focus for the rest of this paper. This period constitutes the northern hemisphere summer, a time when a greater proportion of the land surface receives solar energy amplifying any associated feedback effects. From a paleo-climatic perspective, the temperatures during this period are a key factor in determining whether winter snow and ice can survive through the summer. In view of the page restrictions on this conference paper, the control simulation of 355 ppmv CO_2 with a solar constant of 1367 W m^{-2} is examined with only two other simulations from each of the sensitivity experiments; they are the two outer extremes of +5% and -5% change solar constant experiments and the 180 ppmv and 1000 ppmv CO_2 experiments. It is stressed that the focus of this study is the *sensitivity* of CCM3 to changes in CO_2 and solar luminosity, and not the validation of the model output.

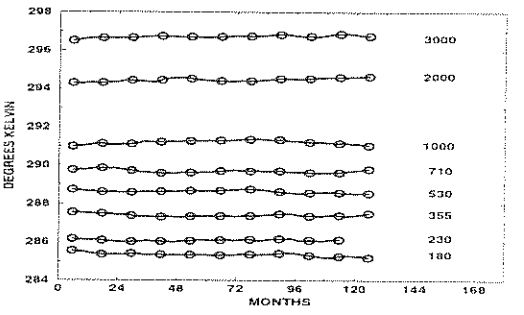

Figure 1: Twelve month running mean for CO_2 simulations. (source: [7]) Numbers to the right of the lines in the plot refer to CO_2 concentrations in ppmv.

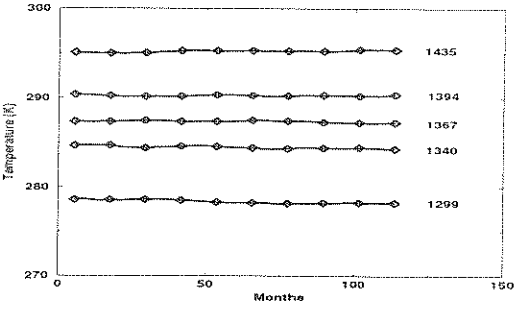

Figure 2: Twelve month running mean for solar constant experiments. Numbers to the right of the lines in the plot refer to the solar luminosity values in W m^{-2}.

The June, July and August (JJA) zonal average temperature profile of the experiments selected for this paper are shown in Figure 3. All simulations show the maximum zonal average temperature at 15°N and warmer zonal average temperatures over the northern hemisphere due to the larger fraction of land mass that warms quicker relative to the ocean and the lack of sea-ice in northern polar latitudes. The two extremes of solar luminosity experiments envelope the control run and the two CO_2 sensitivity experiments implying a greater influence of short-wave forcing on surface temperature compared to the long wave

CO_2 forcing.

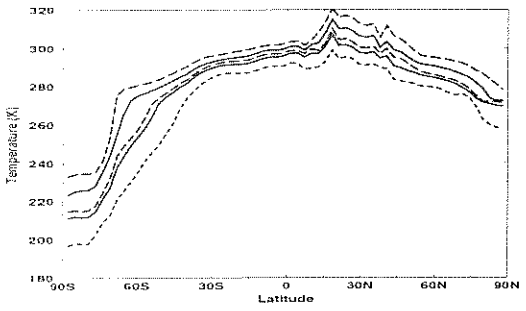

Figure 3: JJA Zonal average temperature for the CO_2 and solar constant runs: -5% solar luminosity (inner dotted line); 180 ppmv CO_2 (inner solid line); 355 ppmv CO_2 (inner dashed line); 1000 ppmv CO_2 (outer solid line); +5% solar luminosity (outer dashed line).

5. Analyses of sensitivities

Figure 4 shows the temperature response for the globe and at 51°N latitude to the aforementioned values of CO_2 for the final five-year ensemble average of June, July and August. Both curves are logarithmic which is similar to the findings of [11] and [13] who used a different GCM. The work of [7] found that sea-ice during the northern hemisphere winter disappeared only at 3000 ppmv.

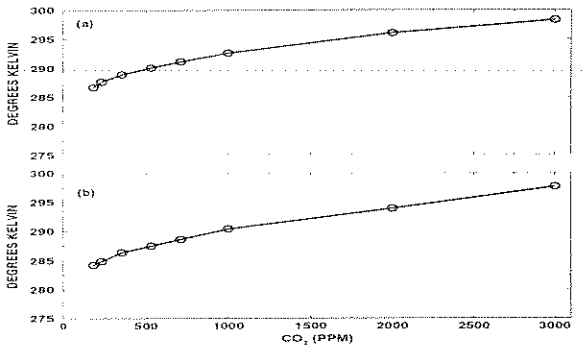

Figure 4: Sensitivity of JJA global-average surface temperature to increasing concentrations of CO_2:(a) global average; (b) 51°N. (source: [7])

On the other hand, the temperature response to changes in solar luminosity is largely linear (Figure 5). It should be noted that the three lines passing through the five points are not a least squares linear regression fit but merely a connection of the JJA global average surface temperature points. A perfect linear fit was obtained through the three points between -2% and +2% changes in the solar constant over the 2849 land points of CCM3. The slope of the line increases between -2% and -5% implying a marginally faster cooling possibly due to the snow-ice albedo feedback. In addition, the slope of the line increases between +2% and +5% which shows the more rapid heating response of land compared to the ocean. The more rapid warming of the land grid points may also be attributed to the drying of soil moisture which leads to the more dominant role of sensible heat and long-wave surface heating to latent heat [9]. This is best illustrated with the warmest curve of Figure 5 showing the sensitivity of the 1626 northern hemisphere land grid points only during June through August.

A less linear fit was obtained over the 5343 ocean grid points (middle line of Figure 5). The reasons for this is the abundance of moisture to saturate the atmosphere just above the ocean surface and the resulting long-wave effects of water vapor - a situation similar to the CO_2 curve.

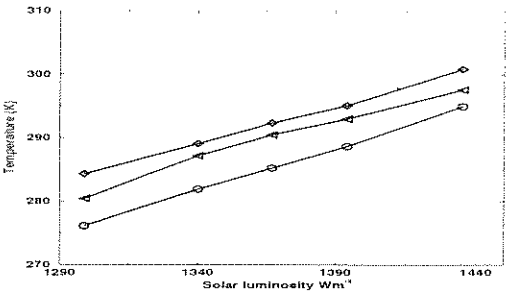

Figure 5: Sensitivity of JJA global-average surface temperature to changes in the solar constant: all land grid points (circles); all ocean grid points (triangles); and northern hemisphere land grid points (diamonds).

6. Geographic anomalies

Figure 6 shows the difference in JJA surface temperature between the 1000 ppmv simulation and the control simulation. The high values around Antarctica, the Hudson Bay and the Arctic circle indicate the melting of sea-ice. The implications of this are an increase in freshwater flux with possible effects on the thermohaline circulation. The maximum increase in surface temperature over the land surface occurs over the Tibetan Plateau possibly due to enhanced snow melt. The interior of continents in the southern hemisphere such as southern Africa and Australia experience milder winters than the present.

Figure 7 shows the difference in surface temperature between the control and the 180 ppmv simulations. The warming here is approximately half in magnitude compared to the previous figure but it is still significant because the CO_2 concentration increased by a factor of two as opposed to a factor of three increase in the previous figure.

Due to the linear sensitivity of CCM3 to changes in solar luminosity, the difference between the 5% increase in solar luminosity and the control simulation (Figure 8)

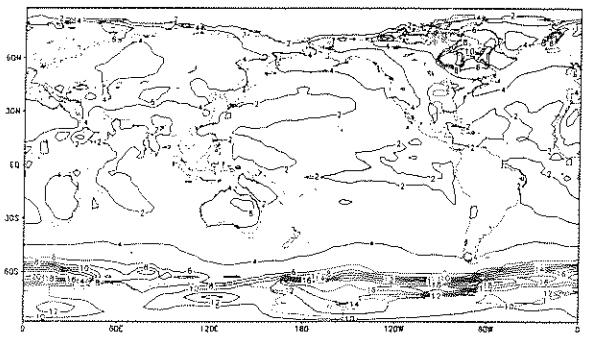

Figure 6: JJA surface temperature (1000 ppmv - control).

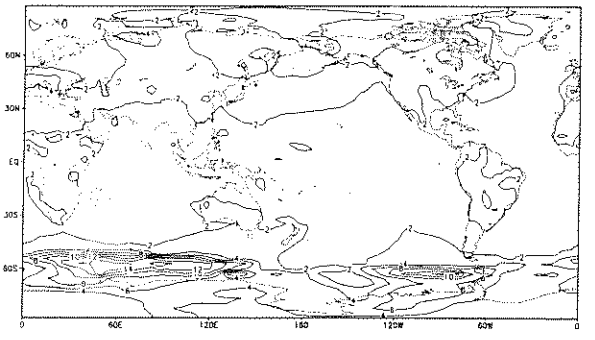

Figure 7: JJA surface temperature (control - 180 ppmv).

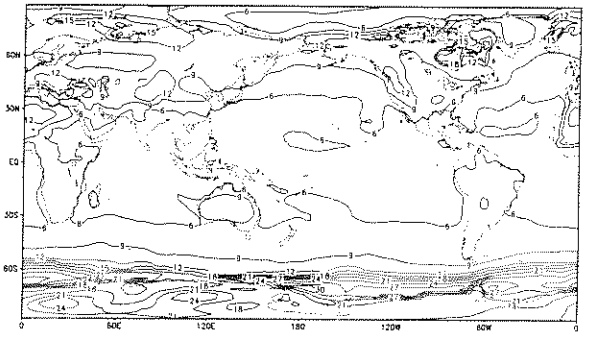

Figure 8: JJA surface temperature (+5% solar constant - control).

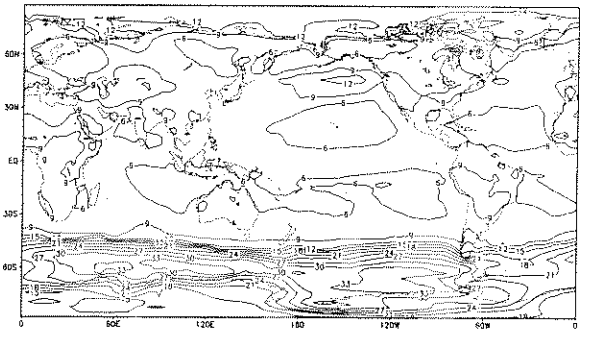

Figure 9: JJA surface temperature (control - -5% solar constant).

shows a larger increase in surface temperature over much of the globe. The greatest warming occurs over the land masses of the winter hemisphere. The 5% increase in solar forcing is likely to melt almost all sea-ice which is evident looking at the magnitude of warming over Antarctica.

Conversely, the difference between in JJA surface temperatures between the control simulation and the 5% decrease in solar luminosity shows larger increases (Figure 9) compared to the previous case in polar latitudes of both hemispheres indicating the dominance of snow and sea-ice. This is also evident from Figure 3 where the innermost zonal average curve of -5% change in solar luminosity is a greater distance away from the control simulation in the southern hemisphere.

In view of the maximum increases in surface temperature around the southern polar latitudes, the difference in the amount of snow cover over Antarctica is examined. Snow occurs when the lowest layers of the model are two degrees below freezing and is a good proxy for examining the combined effects of precipitation with temperature. The anomalies between the 5% increase in solar luminosity and the control run is presented in Figure 10, and the difference between the 5% decrease and the control run in Figure 11. The increase in solar luminosity shows a large melting of snow around the Antarctic peninsula because of the warmer water surrounding this portion of land mass after the melting of sea-ice. The increase in the amount of snow cover over the interior of the Antarctic landmass can be attributed to the warmer atmosphere that can hold more moisture relative to the control climate. This is evident in the differences between the -5% solar constant and the control run (Figure 11) where one finds less snow over the Antarctic landmass.

7. Summary

In summary, the results of the experiments were similar to previous studies and showed a logarithmic response to the long-wave CO_2 forcing and a linear response to the short-wave solar constant forcing. However, the magnitude of the forcings differ. The reasons for the sensitivity curve of CCM3 to increasing CO_2 being different from an earlier version of the model have been discussed by the authors in an earlier paper [7]. They are: a non-local boundary layer scheme; the parameterization of atmospheric convection; the treatment of the implied ocean heat transports; and, the parameterization of long wave radiation. For the solar constant experiments, a least squares linear regression fit through the 8192 horizontal grid points of CCM3 (not shown) has a correlation coefficient of 0.99. An identical experiment using an earlier version of the NCAR CCM (i.e., CCM1) [8] found a linear sensitivity of surface temperature to solar constant changes with a correlation coefficient of 0.96 and a slope

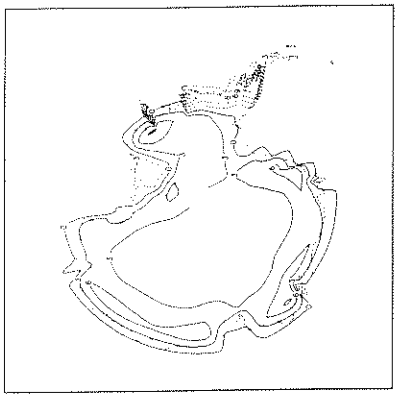

Figure 10: JJA snow (+5% solar constant - control) Contours are at every 3mm of water equivalent.

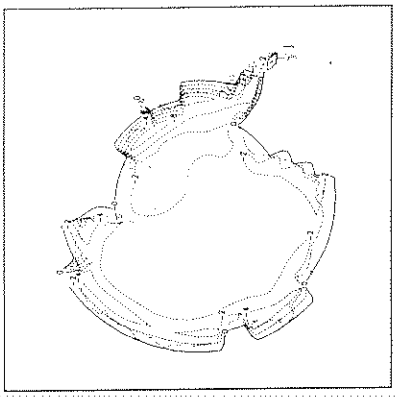

Figure 11: JJA snow (-5% solar constant - control) Contours are at every 2mm of water equivalent.

twice that of CCM3.

The model results to changes in these very different forcings also have profound implications for the hydrologic cycle, water vapor and sea ice feedbacks, all of which are vital for the study of past and future climates. The analysis of these processes are currently being conducted.

Acknowledgements: This research was supported by the United States National Science Foundation (NSF) Climate Dynamics Program grant ATM-9530914. The computations were done at the National Center for Atmospheric Research (NCAR), which is supported by NSF, with computation grant 36211011 from the NCAR Scientific Computing Division.

References

[1] R.A. Berner. GEOCARB II. A revised model of atmospheric CO_2 over Phanerozoic time. *American Journal of Science*, 294:56–91, 1994.

[2] G.B. Bonan. The land surface climatology of the ncar Land Surface Model (LSM 1.0) coupled to the NCAR Community Climate Model (CCM3). *Journal of Climate*, 11:1307–1326, 1998.

[3] J.J. Hack, J.T. Kiehl, and J. Hurrell. The hydrologic and thermodynamic characteristics of the NCAR CCM3. *Journal of Climate*. 11:1179–1206, 1998.

[4] J.T. Houghton, L.G. Meira Filho, B.A. Callander, N. Harris, A. Kattenberg, and K. Maskell, editors. *Climate Change 1995: The Science of Climate Change*. Cambridge University Press, 1996. Contribution of Working Group I to the Second Assessment Report of the Intergovernmental Panel on Climate Change.

[5] G.S. Jenkins. The effects of reduced land fraction and solar forcing on the general circulation - results from the NCAR CCM. *Global and Planetary Change*, 7:321–333, 1993.

[6] J.T. Kiehl, J.J. Hack, G. Bonan, B.A. Boville, D. Williamson, and P. Rasch. The National Center for Atmospheric Research Community Climate Model: CCM3. *Journal of Climate*, 11:1151–1178, 1998.

[7] Z. Kothavala, R.J. Oglesby, and B. Saltzman. Sensitivity of equilibrium surface temperature of CCM3 to systematic changes in atmospheric CO_2. *Geophysical Research Letters*, 26:209–212, 1999.

[8] S. Marshall, R.J. Oglesby, J.W. Larson, and B. Saltzman. A comparison of GCM sensitivity to changes in CO_2 and solar luminosity. *Geophysical Research Letters*, 21:2487–2490, 1994.

[9] R.J. Oglesby. Springtime soil moisture, natural climatic variability and North American drought. *Journal of Climate*, 2:1362–1380, 1991.

[10] R.J. Oglesby and B. Saltzman. Extending the EBM: The effect of deep ocean temperature on climate with applications to the Cretaceous. *Palaeogeography, Palaeoclimatology, Palaeoecology: Global and Planetary Change Section*, 82:237–259, 1990.

[11] R.J. Oglesby and B. Saltzman. Sensitivity of the equilibrium surface temperature of a GCM to systematic changes in atmospheric carbon dioxide. *Geophysical Research Letters*, 17:1089–1092, 1990.

[12] L.C. Sloan and D.K. Rea. Atmospheric carbon dioxide and early Eocene climate: A general circulation modeling sensitivity study. *Palaeogeography, Palaeoclimatology, Palaeoecology*, 119:275–292, 1995.

[13] J. Syktus, H. Gordon, and J. Chappell. Sensitivity of a coupled atmosphere-dynamic upper ocean GCM to variations of CO_2, solar constant, and orbital forcing. *Geophysical Research Letters*, 21:1599–1602, 1994.